Supplementary Information for "Upstream Mobility and Swarming of Light Activated Micromotors"

Bingzhi Wu,[1] David P. Rivas,[1] and Sambeeta Das[1]
[1] *Department of Mechanical Engineering, Newark, DE, USA, 19716*

I. LIST OF SUPPLEMENTARY VIDEOS

Video S1: A video of several examples of the upstream mobility of the micromotors with applied UV light. The final example includes a circle around the micromotor for visual aid.
Video S2: A micromotor swarm in dynamic equilibrium at the light boundary. The flow is left to right. The typical micromotor in the non-illuminated region moves with the flow at around 32 μm/s and up to approximately 100 μm/s.
Video S3: Examples of moving the swarms upstream and downstream. Moving the light downstream of the swarm results in the micromotors moving with the flow downstream until they reach the light where they attain sufficient speed to swim against the flow. Moving the light upstream of the swarm supplies more light intensity to the micromotors and allows them to propagate upstream towards the new position of the light boundary.
Video S4: An example of the motion of the micromotors in a channel with very low flow.
Video S5: An example of the micromotors leaving the edges of the channel and moving downstream with the flow after the light is turned off.
Video S6: An example of the motion of the swarm of micromotors immediately after the light was turned off and the micromotors move with the fluid flow. The micromotors increase their speed over time, indicating that they were initially near the channel boundary where the flow is somewhat reduced.

II. MATERIALS AND METHODS

A. Fabrication of the Light Activated Micromotors

The light active motors were made by first mixing tetrabutyl titanate (Sigma #244112) with ethanol at a 1/40 ratio. The mixture was allowed to sit for one day then the solution was centrifuged at 7000 rpm (Eppendorf 5415) for 1 minute to remove the supernatant. This resulted in particle diameters of approximately 1.5-2.5 μm. The micromotors were rinsed a total of three times in ethanol and three times in DI water. A glass vial containing the motors were placed on a hot plate at approximately 90°C to evaporate the water. The dry motors were then placed in a furnace at 400°C to create the anatase phase. They were then re-suspended in ethanol and spread evenly onto a glass slide. After evaporation, the motors were coated in Ni/Fe alloy, Pt, and then Ag by electron-beam evaporation. The Ni/Fe layer made the motors magnetically responsive while the Pt and Ag layers were added to improve their light responsiveness. Previous studies have shown the high effectiveness of using Pt to increase the speed of TiO2 micromotors compared to other metals [1], and other studies have shown that a bimetal coating can be advantages as well [2]. Using an outer Ag layer rather than Pt also reduces the catalytic decomposition of hydrogen peroxide which reduces the problem of oxygen bubble formation in the channels. The coating thickness of the layers were all 20nm. The Ni/Fe layer was coated at a glancing angle of 20 degrees (70 degrees from normal) in order to reduce the amount on the spheres and therefore increase the surface contact with Pt.

B. Microfluidic Channel Fabrication

The microfluidic channels were made using standard photolithography techniques. The design of the microchannels was made in AutoCAD and a plastic photomask was purchased from Fine-Line Imaging (Colorado Springs, CO) at a resolution of 7 μm. The micorchannels were designed with a width of 35 μm, a height of 16 μm, and a length of 1.5 cm. A photoresist, SU8-2010, was pipetted onto a silicon wafer while it was rotated at 500 rpm on a spin coater. After depositing the photoresist such that it covered the wafer, the spinning rate was then accelerated to 1500 rpm and maintained for 30s in order to obtain an ultimate thickness of 16 μm. A prebake at 65°C for 1 minute and 95°C for 4 minutes was used to evaporate the solvent. The photoresist was then exposed at a dose of 140 mJ/cm2 using a mask aligner (NXQ8006). A post-exposure bake whose recipe was the same as that for pre-bake was then applied. The slide was developed by submerging it in SU8 developer for 3 minutes.

The wafer was placed into a container which was filled with polydimethylsiloxane (PDMS, formed by mixing SYLGARD 184 Silicone Elastomer Base and a curing agent in a mass ratio of 10:1) after the photoresist was secured on the wafer. The container was then placed on a hot plate and heated at 70°C for 2 hours in order to vaporize the redundant solvent. The PDMS was then cut into pieces using a razor such that there were two parallel channels per piece. A glass slide and the PDMS were placed into a plasma cleaner (PDC-00)1 for

3 minutes. The treated side of the PDMS was then immediately placed in contact with the treated side of the glass slide once the plasma cleaning process was done to form a strong adhesion between the PDMS and glass.

C. Experimental Procedures

The experiments were observed and recorded under a microscope (ZEISS Axiovert 200) with 20x objective and used a digital micromirror device (DMD) as the UV light source (MIGHTEX Polygon 1000 Pattern Illuminator), which produces a peak UV intensity at 365 nm. We used an intensity of around 500 mW/cm^2. A schematic of the experimental setup is shown in Fig. 1. The micromotors were removed from their glass substrate using a wet lens tissue which was wiped along the slide to pick up the motors and then placed in a vial with DI water and vortexed. The tissue was then removed, leaving the motors suspended in the vial. Approximately 1 mL of the particle solution was made, and hydrogen peroxide was added to the solution to make a final concentration of 0.6, 1.15, or 1.7 vol%. The solution was then sonicated for 30 seconds. The mixture was transferred into a 1 mL syringe which was then connected to tubes that were inserted into the microchannel inlet. The syringe was mounted onto a syringe pump (Chemyx Fusion 200) and another empty syringe was also attached to the outlet side of the channel and connected to an identical pump. The two syringe pumps were simultaneously turned on such that they both injected the solution while removing the air from the channel at a constant rate of approximately 0.005 mL/min. Once the solution of motors filled the channel, the pump was turned off and the inlet and outlet tubes were disconnected from both ends of the channel in order to reduce the flow rate. We find that a steady flow developed which would last for up to an hour before slowing down further or changing direction. We speculate that the flows were due to uneven pressure caused by evaporation at the inlet and outlet of the channels. To increase the flow rate, the tubes could be reconnected and the pumps turned back on, and subsequently turned off again and the tubes removed. A magnetic field was applied by placing a permanent magnetic a few centimeters from the microchannel. The magnetic field causes the active micromotors to move in more linear trajectories compared to when no field is applied. Even when a magnetic field was applied, the direction of motion of the micromotors remained arbitrary and did not follow a parallel path with the field, which we attribute to differences in the magnetic coatings on the microspheres caused by the glancing angle deposition on the polydisperse and dense layer of microspheres on the substrate.

D. Particle Tracking and Statistical Analysis

To track the motors and extract their velocities, videos were analyzed in Python using Trackpy particle tracking software [3]. The velocities were determined by taking the derivative of the x and y position of the motors after smoothing. All the uncertainties were estimated by calculating the standard error of the mean.

To calculate the velocity profile within the channel, the channel was divided into 7 equally spaced sections and the motors' average speeds were found within each of these regions. The ensemble average and standard error of these individual averages were then found to obtain the velocity profile as shown in Fig. S1.

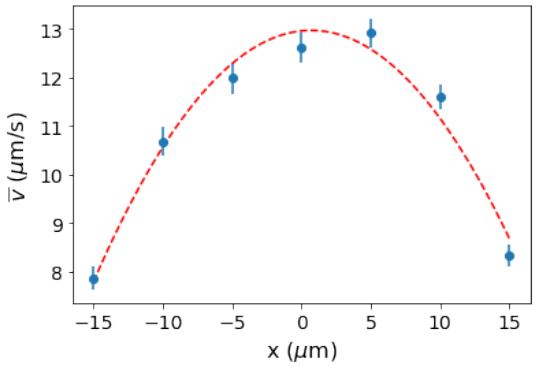

Fig. S1. The velocity profile within a microchannel, as found by measured the flow velocity of tracer particles in the fluid, along with a parabolic fit to the data. The mean velocity was computed within each of the 7 equally spaced 5 μm wide regions over the 35 μm wide channel.

E. Micromotor Speed Vs Light and Fuel Concentration

The micromotor speed as a function of light intensity and hydrogen peroxide fuel concentration was measured and the result is shown in Fig. S2. Suspended micromotors were pipetted onto glass substrates and their trajectories were found using particle tracking software in a similar manner to that described above.

Since the micromotors had a large variation of speed and only the fastest ones were able to overcome the flow and form the swarms, we measured the speed of the fastest micromotor (out of approximately 20 micromotors in the field of view) and computed an average over multiple trials. Since the micromotors would sometimes stick to the slide for some time while the light was on, we computed the maximal speed rather than the average since we believe this more accurately represents their speed when they are freely moving.

As can be seen from the plot, the micromotors generally moved faster with higher light intensity, as expected,

and show a weak dependence on fuel concentration between 0.5 and 2 percent.

[1] T. Maric, M. Z. M. Nasir, R. D. Webster, and M. Pumera, Tailoring metal/tio2 interface to influence motion of light-activated janus micromotors, Advanced Functional Materials **30**, 1908614 (2020), https://onlinelibrary.wiley.com/doi/pdf/10.1002/adfm.201908614

[2] Z. Xiao, J. Chen, S. Duan, X. Lv, J. Wang, X. Ma, J. Tang, and W. Wang, Bimetallic coatings synergistically enhance the speeds of photocatalytic tio2 micromotors, Chem. Commun. **56**, 4728 (2020).

[3] D. B. Allan, T. Caswell, N. C. Keim, C. M. van der Wel, and R. W. Verweij, soft-matter/trackpy: Trackpy v0.5.0 (2021).

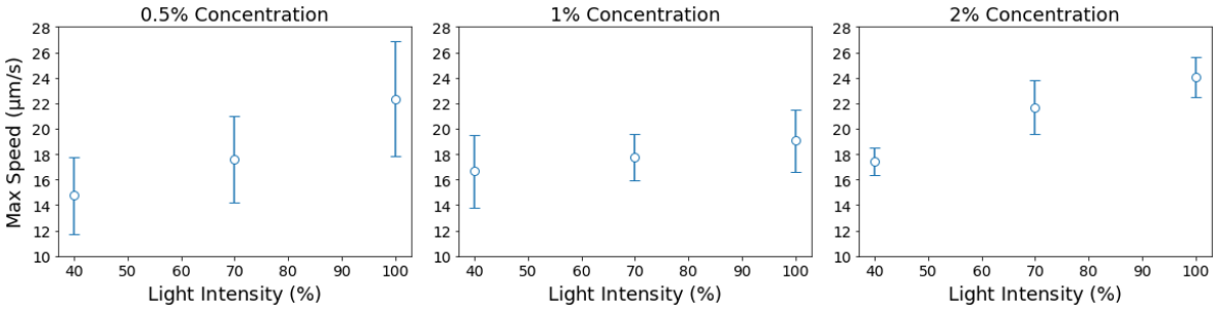

Fig. S2. The measured maximal micromotor speed, averaged over multiple trials of about 20 micromotors in each trial, as a function of light intensity and fuel concentration.